

DESY-96-103

MC-TH-96/18

June 1996

Further analysis of the BFKL equation with momentum cutoffs

M.F.McDermott¹

and

J.R.Forshaw²¹ DESY, Theory Group, Notkestr. 85, 22607 Hamburg, Germany² Dept. of Physics and Astronomy, The University of Manchester, Manchester,
England M13 9PL

Abstract

In this paper we investigate the effect of introducing transverse momentum cutoffs on the BFKL equation. We present solutions in moment space for various models of the BFKL kernel for different combinations of these cutoffs. We improve on previous calculations by using the full BFKL kernel (rather than simplified analytic approximations). The significance of the next-to-leading or “higher twist” terms in the kernel are assessed. We find that, while these terms are negligible in the absence of cutoffs, introducing an infra-red cutoff markedly enhances their significance.

1 Introduction

The BFKL equation [1] can be formulated as an integral equation which determines the evolution (in x) of the unintegrated gluon distribution function $f(x, k^2)$. It is expected to be relevant for sufficiently small x , (i.e. $\alpha_s \ln 1/x \sim 1$) providing the, as yet unquantified, sub-leading corrections are not too large. Cross-sections which are sensitive to the small- x dynamics are constructed by convoluting $f(x, k^2)$ with the appropriate coefficient functions (impact factors). In this paper we consider the integrated structure function

$$\int_0^{Q^2} \frac{dk^2}{k^2} f(x, k^2) \equiv G(x, Q^2), \quad (1)$$

which is equivalent to the usual DGLAP [2] gluon density, $xg(x, Q^2)$, in the double leading logarithm approximation. However, this is not a physical observable and computation, for example, of the deep inelastic structure functions $F_2(x, Q^2)$ and $F_L(x, Q^2)$ requires less trivial integrals over k^2 .

Here we do not consider the phenomenologically more interesting cross-sections. Rather, we wish to elucidate more on the technical details which are involved in computing $G(x, Q^2)$ using a modified BFKL kernel. Our modifications correspond to restricting the virtualities of the t -channel gluons in the real emission part of the BFKL kernel, in line with possible constraints imposed by energy conservation and the desire to keep away from the region of low virtualities, i.e. *we impose fixed infra-red and ultra-violet cut-offs on the real emission part of the kernel*. We introduce these phase-space restrictions on the full BFKL kernel.

First recall the (angular averaged) BFKL equation for the evolution of the (unintegrated) gluon density. It may may be written

$$f(x, k^2) = f^{(0)}(x, k^2) + \frac{3\alpha_s k^2}{\pi} \int_x^{x_0} \frac{dx'}{x'} \int_0^\infty \frac{dk'^2}{k'^2} \times \left\{ \frac{(f(x', k'^2) - f(x', k^2))}{|k'^2 - k^2|} + \frac{f(x', k^2)}{\sqrt{k^4 + 4k'^4}} \right\}. \quad (2)$$

Although this equation has been known for some time there are various theoretical difficulties in determining its phenomenological implications. The equation is derived in a limit where α_s is kept fixed, and only includes leading terms (i.e.

terms with equal powers of α_s and $\ln(1/x)$). Furthermore, the equation involves an integration over *all transverse momenta* including the lowest values where perturbation theory is expected to break down (because large radiative corrections lead to $\alpha_s > 1$). This region may be regulated by introducing an infra-red cutoff [3, 4, 5]. In addition, energy conservation demands that an ultra-violet cutoff is present [6]. The purpose of this paper is to determine the effect that these cutoffs have on the mathematical structure of the equation and its solution.

Clearly in order to produce a realistic model of a small x physical cross section some attempt must be made to parameterize the region of phase space which we have removed (below the infra-red cutoff) where confinement effects are expected to become important. Some phenomenological attempts have been made in this direction [3, 5]. In this paper we restrict ourselves to a consideration of what we feel may be reliably calculated within the framework of perturbative QCD and make no attempt to discuss what happens outside of this region.

The equation is best solved by taking Mellin moments with respect to x, k^2 defined by

$$f(x, k^2) = \int_{c-i\infty}^{c+i\infty} \frac{d\omega}{2\pi i} (k^2)^{\omega+\frac{1}{2}} \tilde{f}(x, \omega) \quad (3)$$

$$\tilde{f}(x, \omega) = \int_0^\infty dk^2 (k^2)^{-\frac{3}{2}-\omega} f(x, k^2) \quad (4)$$

$$\tilde{f}(x, \omega) = \int_{c-i\infty}^{c+i\infty} \frac{dN}{2\pi i} x^N \mathcal{F}(N, \omega) \quad (5)$$

$$\mathcal{F}(N, \omega) = \int_0^1 dx x^{-1-N} \tilde{f}(x, \omega). \quad (6)$$

The contour in eq.(5) lies parallel to the imaginary axis and to the left of all singularities in the N -plane. In eq.(3) the contour also lies parallel to the imaginary axis and to the left of all singularities associated with the small k^2 behaviour of $f(x, k^2)$ but to the right of singularities associated with its large k^2 behaviour. This choice ensures that the respective inverses of these transforms exist and are consistent. The addition of $1/2$ to the power of k^2 included in eq.(3) is merely for convenience. With this definition the ω -plane contour lies along $\Re(\omega) = 0$.

The following solution to the BFKL equation (in ‘Double Mellin Transform’ space) is then obtained:

$$\mathcal{F}(N, \omega) = \frac{\mathcal{F}^{(0)}(N, \omega)}{(1 + N^{-1}K(\omega))}. \quad (7)$$

where $K(\omega)$ is the (Mellin transform of the) BFKL kernel

$$K(\omega) = \bar{\alpha}_s[-2\gamma - \psi(\frac{1}{2} + \omega) - \psi(\frac{1}{2} - \omega)] = \bar{\alpha}_s\chi(\omega), \quad (8)$$

ψ and γ are the logarithmic derivative of the gamma function and the Euler constant respectively and $\bar{\alpha}_s \equiv 3\alpha_s/\pi$. The full kernel has an infinite set of simple poles at $\omega = \{ \pm 1/2, \pm 3/2, \dots \}$ as a result of the poles in the ψ functions. Fig.(1) shows the real part of the kernel in the region of interest closest to the contour.

In a previous paper [7] we presented a method for finding $\mathcal{F}(N, \omega)$ in the presense of infra-red, Q_0^2 , and ultra violet, Q_1^2 , transverse momentum cutoffs on the real terms (i.e. the $f(x, k^{2'})$ terms) in eq.(2)) for a general input distribution $\mathcal{F}^{(0)}(N, \omega)$. The results may be summarised as follows:

$$\mathcal{F}(N, \omega) = \frac{1}{(1 + N^{-1}K(\omega))}(\mathcal{F}^{(0)}(N, \omega) + \mathcal{S}(N, \omega)). \quad (9)$$

The function $\mathcal{S}(N, \omega)$ depends in general on Q_0^2 and Q_1^2 , and upon the parameterisation chosen for the input distribution. Explicitly we considered three cases: the non-cutoff case, the single (infra-red) cutoff case and the double (infra-red and ultra-violet) cutoff case (hereafter denoted with a subscript n , s and d , respectively). $\mathcal{S}_s(N, \omega)$ is uniquely determined by the fact that it must cancel all poles from $\mathcal{F}_s(N, \omega)$ to the right of the contour in the ω -plane. Similarly $\mathcal{S}_d(N, \omega)$ must cancel all poles to the right and to the left of the contour. The structure of the solutions in (x, k^2) -space depend on the pole structure in Mellin space, the positions of which are determined by the zeros of the denominator of eq.(9):

$$N + K(\omega) = 0. \quad (10)$$

In this paper we present solutions in (N, k^2) -space for various models of the kernel and cutoff combinations. Initially we consider a simplified model for the kernel, introduced by Collins and Landshoff [4], in which only the two poles

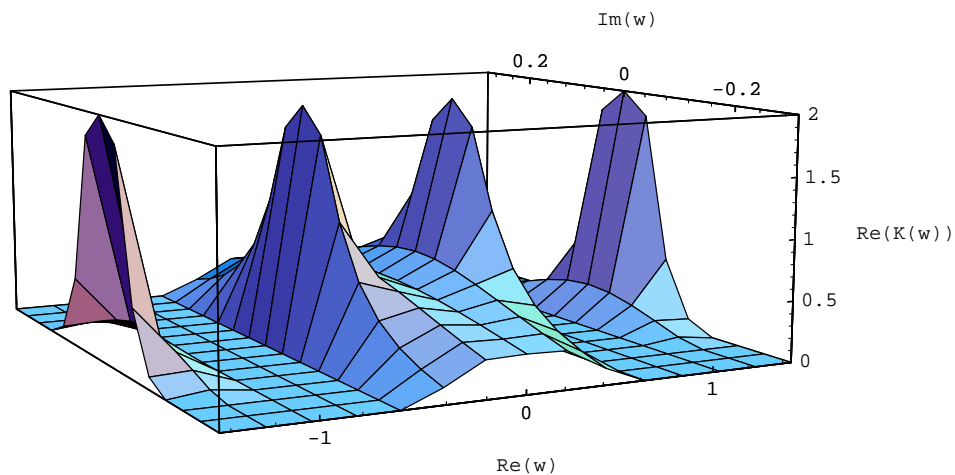


Figure 1: Real part of the BFKL kernel for $\bar{\alpha}_s = 0.2$. Note the saddle point at $\omega = (0, 0)$ and the poles at $\omega = \pm\frac{1}{2}, \pm\frac{3}{2}, \dots$. The poles in $\mathcal{F}(N, \omega)$ in the ω -plane are given by the solution to $N + K(\omega) = 0$.

nearest to the contour in eq.(3) are kept. These are the poles which lead to the dominant behaviour of $G(x, Q^2)$ in the limit $Q^2 \rightarrow \infty$. We present solutions for a particular input distribution, chosen such that its parameters are distinct from those subsequently used for the cutoffs on the BFKL evolution. We repeat the analysis implementing the exact kernel of eq.(8), again keeping only the leading ω -plane poles. The integration over the k^2 is performed in N -moment space and the results are presented in terms of the moment of the integrated gluon distribution $G(N, Q^2)$ [8, 9] for each case. We present the effective small- x slope in each scenario.

The inclusion of additional (“higher twist”) ω -plane poles in the kernel is then implemented (i.e. the two nearest poles on each side of the contour in eq.(3)). Their numerical significance (as a function of x and Q^2) is assessed. Again we use the full BFKL kernel.

For the case with no cutoffs present we find that the small- x behaviour, even for fairly low values of Q^2 , is dominated by the leading pole in the ω -plane (the next-to-leading poles contribute less than 1% for $x < 10^{-3}$). That we can safely neglect all poles other than the two which lie nearest the ω -plane contour is essential for the validity of the DGLAP formulation of the small- x structure functions (e.g. see [8, 9, 10, 11, 12]).

In the presence of infra-red cutoff the addition of the subleading pole (there is only one pole to add for an infra-red cutoff) has a more significant effect. We present results on the size of this effect as a function of x and Q^2 and comment on its possible significance. We find that the next-to-leading terms may be as large as $\approx 20\%$ for moderate values of Q^2 .

2 The simple model revisited

Let us briefly recap the examples given in [7]. The following two pole model for the kernel was used

$$K(\omega) = \frac{4 \ln 2\bar{\alpha}_s}{(1 - 4\omega^2)} = \frac{K_0}{(1 - 4\omega^2)}. \quad (11)$$

for which eq.(10) has only two solutions which we denote $\pm\omega_{N1}$, where

$$\omega_{N1} = \frac{1}{2}\sqrt{1 + \frac{K_0}{N}} \quad (12)$$

$$\frac{1}{1 + N^{-1}K(\omega)} = \frac{\omega^2 - \frac{1}{4}}{\omega^2 - \omega_{N1}^2}. \quad (13)$$

In the infra-red cutoff case $\mathcal{S}_s(N, \omega)$ removes the pole at $\omega = \omega_{N1}$, i.e. it satisfies

$$\mathcal{F}^{(0)}(N, \omega_{N1}) + \mathcal{S}_s(N, \omega_{N1}) = 0. \quad (14)$$

So, the solution is given by

$$\begin{aligned} \mathcal{F}_s(N, \omega) &= \frac{1}{1 + N^{-1}K(\omega)} \times \\ &\left(\mathcal{F}^{(0)}(N, \omega) + \frac{\mathcal{F}^{(0)}(N, \omega_{N1})\left(\frac{1}{2} - \omega_{N1}\right)Q_0^{-2(\omega - \omega_{N1})}}{\omega - \frac{1}{2}} \right) \end{aligned} \quad (15)$$

for $k^2 > Q_0^2$ and zero otherwise.

In the double cutoff case $\mathcal{S}_d(N, \omega)$ removes both poles in eq.(13), i.e. it also satisfies

$$\mathcal{F}^{(0)}(N, -\omega_{N1}) + \mathcal{S}_d(N, -\omega_{N1}) = 0, \quad (16)$$

and the solution is given by

$$\begin{aligned} \mathcal{F}_d(N, \omega) &= \frac{1}{1 + N^{-1}K(\omega)} \times \\ &\left[\mathcal{F}^{(0)}(N, \omega) + \frac{1}{\Delta(\omega_{N1})} \{ \Delta(\omega_{N1})\mathcal{S}(N, \omega) \} \right], \end{aligned} \quad (17)$$

for $Q_0^2 < k^2 < Q_1^2$ and zero otherwise, where

$$\begin{aligned} \Delta(\omega_{N1})\mathcal{S}(N, \omega) &= \frac{Q_0^{-2\omega}}{(\omega - \frac{1}{2})} \\ &\times \left[\left(\frac{1}{2} + \omega_{N1}\right)Q_1^{2\omega_{N1}}\mathcal{F}^{(0)}(N, \omega_{N1}) - \left(\frac{1}{2} - \omega_{N1}\right)Q_1^{-2\omega_{N1}}\mathcal{F}^{(0)}(N, -\omega_{N1}) \right] \\ &+ \frac{Q_1^{-2\omega}}{(\omega + \frac{1}{2})} \end{aligned}$$

$$\times \left[\left(\frac{1}{2} - \omega_{N1} \right) Q_0^{2\omega_{N1}} \mathcal{F}^{(0)}(N, \omega_{N1}) - \left(\frac{1}{2} + \omega_{N1} \right) Q_0^{-2\omega_{N1}} \mathcal{F}^{(0)}(N, -\omega_{N1}) \right], \quad (18)$$

$$\Delta(\omega_{N1}) = \frac{\frac{1}{2} + \omega_{N1}}{\frac{1}{2} - \omega_{N1}} (Q_1^2/Q_0^2)^{\omega_{N1}} - \frac{\frac{1}{2} - \omega_{N1}}{\frac{1}{2} + \omega_{N1}} (Q_1^2/Q_0^2)^{-\omega_{N1}} \quad (19)$$

In [4] a simple powerlike input distribution in k^2 (truncated at the scale of the limits of the evolution integration over k^2) is used, i.e. the inputs are

$$f_s^{(0)}(x, k^2) = A x^{-\epsilon} (k^2)^{(\omega_0+1/2)} \Theta(k^2 - Q_0^2) \quad (20)$$

$$\mathcal{F}_s^{(0)}(N, \omega) = \frac{A Q_0^{2(\omega_0-\omega)}}{(N+\epsilon)(\omega_0-\omega)} \quad (21)$$

$$f_d^{(0)}(x, k^2) = A x^{-\epsilon} (k^2)^{(\omega_0+1/2)} \Theta(k^2 - Q_0^2) (1 - \Theta(k^2 - Q_1^2)) \quad (22)$$

$$\mathcal{F}_d^{(0)}(N, \omega) = \frac{A(Q_0^{2(\omega_0-\omega)} - Q_1^{2(\omega_0-\omega)})}{(N+\epsilon)(\omega_0-\omega)}. \quad (23)$$

The dimensionless input distribution has normalisation A (which carries dimensions $[-(\omega_0 + 1/2)]$), $\omega_0 < 1/2$ ensuring that its momentum distribution dies off at large k^2 and $\epsilon \sim 0.08$ gives an x dependence motivated by the observed slow rise of the proton-antiproton total cross section at high energies (see e.g. [13]). With these choices of input distribution eqs.(15,17) agree with those derived in [4] upto a minus sign (for the latter) as described in [7].

For later convenience we rewrite eq.(18) as

$$\Delta(\omega_{N1}) \mathcal{S}(N, \omega) = \frac{A}{N+\epsilon} \left(\frac{Q_0^{-2\omega} X_1(\omega_{N1})}{(\omega - \frac{1}{2})} + \frac{Q_1^{-2\omega} X_2(\omega_{N1})}{(\omega + \frac{1}{2})} \right) \quad (24)$$

where X_1, X_2 are given by the terms in square brackets in eq.(18) with the $A/(N+\epsilon)$ factor removed.

We now investigate the sensitivity of this model to the degeneracy of the upper and lower scales used to parameterise the input distribution and those employed to restrict the k^2 integrals in the evolution equation. Explicitly we replace Q_0^2, Q_1^2 in eqs.(21,23) with μ_0^2, μ_1^2 . By keeping these scales distinct and using the same input in each case we demonstrate the smooth matching between the solutions as $Q_0^2 \rightarrow 0, Q_1^2 \rightarrow \infty$. A comprehensive series of analytic and numerical cross checks are performed which give us confidence in the solutions.

However there is a more important reason for making this distinction. Physically we expect the input distribution to be peaked around small values of k^2 with a small tail in the perturbative high- k^2 region. It is these perturbative gluons which we may justifiably evolve in perturbative QCD using the BFKL equation. For convenience we choose to use a theta function to model the input, thereby restricting ourselves to the high- k^2 gluons above some scale. Hitherto we have not made the distinction between this scale and the infra-red cutoff scale on the integral of the BFKL equation (which defines how the input distribution evolves with x). This is clearly an unphysical restriction since the choice of input should be independent of how we choose to model the kernel.

We proceed now with the simple model in which these two scales are kept distinct. For generality, we now choose to use input $\mathcal{F}_s^{(0)}$ in the non-cutoff case too. We assume for the time being that $\mu_0^2 > Q_0^2$ since we are interested in taking the limit $Q_0^2 \rightarrow 0$.

The ω -plane contour of eq.(3) is closed in either the left or right half plane according to the behaviour demanded by the ‘‘closure factor’’ in the integrand. In the non-cutoff case the closure factor, $(k^2/\mu_0^2)^\omega$, forces closure to the left for $k^2 > \mu_0^2$ and gives

$$\tilde{f}_n(N, k^2) = \frac{A}{(N + \epsilon)} \left(-\frac{k^{2(1/2+\omega_0)}}{(1 + N^{-1}K(\omega_0))} + \frac{k^{2(1/2-\omega_{N1})}\mu_0^{2(\omega_0+\omega_{N1})}(\frac{1}{4} - \omega_{N1}^2)}{2\omega_{N1}(\omega_0 + \omega_{N1})} \right) \quad (25)$$

and to the right for $k^2 < \mu_0^2$

$$\tilde{f}_n(N, k^2) = \frac{A}{(N + \epsilon)} \left(\frac{(\frac{1}{4} - \omega_{N1}^2)k^{2(1/2+\omega_{N1})}\mu_0^{2(\omega_0-\omega_{N1})}}{2\omega_{N1}(\omega_0 - \omega_{N1})} \right). \quad (26)$$

In the single-cutoff case the factor $(k^2/\mu_0^2)^\omega$ enforces closure to the left for the region $k^2 > \mu_0^2 > Q_0^2$ to give

$$\tilde{f}_s(N, k^2) = \frac{A}{(N + \epsilon)} \left(-\frac{k^{2(1/2+\omega_0)}}{(1 + N^{-1}K(\omega_0))} + \frac{k^{2(1/2-\omega_{N1})}(\frac{1}{2} - \omega_{N1})}{2\omega_{N1}} \times \left[\frac{(\frac{1}{2} + \omega_{N1})\mu_0^{2(\omega_0+\omega_{N1})}}{(\omega_0 + \omega_{N1})} - \frac{(\frac{1}{2} - \omega_{N1})\mu_0^{2(\omega_0-\omega_{N1})}(Q_0^2)^{2\omega_{N1}}}{(\omega_0 - \omega_{N1})} \right] \right) \quad (27)$$

and to the right for $\mu_0^2 > k^2 > Q_0^2$

$$\begin{aligned} \tilde{f}_s(N, k^2) = & \frac{A}{(N + \epsilon)} \frac{(\frac{1}{2} - \omega_{N1}) \mu_0^{2(\omega_0 - \omega_{N1})}}{2\omega_{N1}(\omega_0 - \omega_{N1})} \times \\ & \left((\frac{1}{2} + \omega_{N1}) k^{2(1/2 + \omega_{N1})} - (\frac{1}{2} - \omega_{N1}) k^{2(1/2 - \omega_{N1})} (Q_0^2)^{2\omega_{N1}} \right). \end{aligned} \quad (28)$$

Similarly the double cutoff case solution is given by

$$\begin{aligned} \tilde{f}_d(N, k^2) = & \frac{A}{(N + \epsilon)} \left(-\frac{k^{2(1/2 + \omega_0)}}{(1 + N^{-1}K(\omega_0))} \right. \\ & + \frac{k^{2(1/2 - \omega_{N1})}(\frac{1}{2} - \omega_{N1})}{2\omega_{N1}} \\ & \times \left[\frac{(\frac{1}{2} + \omega_{N1}) \mu_0^{2(\omega_0 + \omega_{N1})}}{(\omega_0 + \omega_{N1})} - \frac{Q_0^{2\omega_{N1}} X_1(\omega_{N1})}{\Delta(\omega_{N1})} \right] \\ & + \frac{k^{2(1/2 + \omega_{N1})}(\frac{1}{2} - \omega_{N1})}{2\omega_{N1}} \\ & \times \left. \left[-\frac{(\frac{1}{2} + \omega_{N1}) \mu_1^{2(\omega_0 - \omega_{N1})}}{(\omega_0 - \omega_{N1})} + \frac{Q_1^{-2\omega_{N1}} X_2(\omega_{N1})}{\Delta(\omega_{N1})} \right] \right) \end{aligned} \quad (29)$$

for $k^2 > \mu_0^2 > Q_0^2$,

$$\begin{aligned} \tilde{f}_d(N, k^2) = & \frac{A}{(N + \epsilon)} \frac{(\frac{1}{2} - \omega_{N1})}{2\omega_{N1}} \left(\frac{k^{2(\frac{1}{2} + \omega_{N1})}(\frac{1}{2} + \omega_{N1})(\mu_0^{2(\omega_0 - \omega_{N1})} - \mu_1^{2(\omega_0 - \omega_{N1})})}{(\omega_0 - \omega_{N1})} \right. \\ & \left. + k^{2(\frac{1}{2} + \omega_{N1})} Q_1^{-2\omega_{N1}} \frac{X_2(\omega_{N1})}{\Delta(\omega_{N1})} - k^{2(\frac{1}{2} - \omega_{N1})} Q_0^{2\omega_{N1}} \frac{X_1(\omega_{N1})}{\Delta(\omega_{N1})} \right) \end{aligned} \quad (30)$$

for $\mu_0^2 > k^2 > Q_0^2$, and

$$\begin{aligned} \tilde{f}_d(N, k^2) = & -\frac{A}{(N + \epsilon)} \left(\frac{k^{2(1/2 - \omega_{N1})}(\frac{1}{4} - \omega_{N1}^2)}{2\omega_{N1}} \left[\frac{\mu_0^{2(\omega_0 + \omega_{N1})} - \mu_1^{2(\omega_0 + \omega_{N1})}}{(\omega_0 + \omega_{N1})} \right] + \right. \\ & \frac{(\frac{1}{2} - \omega_{N1})}{2\omega_{N1}} \times \\ & \left. \left(k^{2(1/2 - \omega_{N1})} Q_0^{2\omega_{N1}} \frac{X_1(\omega_{N1})}{\Delta(\omega_{N1})} - k^{2(1/2 + \omega_{N1})} Q_1^{-2\omega_{N1}} \frac{X_2(\omega_{N1})}{\Delta(\omega_{N1})} \right) \right) \end{aligned} \quad (31)$$

for $Q_1^2 > k^2 > \mu_1^2 > \mu_0^2 > Q_0^2$ and X_1, X_2 are defined in eq.(24). $\tilde{f}_d(N, k^2)$ is the most general solution in that it uses the most general input distribution and contains the solutions in the other cases.

At first the solutions derived above seem very complicated. However one may check that they are indeed correct by looking at the solutions in various limits. With the definition (12) of ω_{N1} as the positive square root we have that $\Re(\omega_{N1}) > 0$ along the contour. We will use this result in what follows. First we look at f_s in the distinct cutoff case. If we take $\mu_0^2 = Q_0^2$ in eq.(27) we obtain

$$\tilde{f}_s(N, k^2) = \frac{1}{(1 + N^{-1}K(\omega_0))} \left(-\frac{Ak^{2(1/2+\omega_0)}}{(N+\epsilon)} + \frac{Ak^{2(1/2-\omega_{N1})}(\frac{1}{2} - \omega_{N1})}{(N+\epsilon)(\omega_0 + \frac{1}{2})} \right) \quad (32)$$

which is precisely what one would obtain upon inverting eq.(19) of [4]. In the limit $Q_0^2 \rightarrow 0$ eqs.(27,28) tend to eqs.(25,26). So we have

$$\lim_{\mu_0^2 \rightarrow Q_0^2} \tilde{f}_s(N, k^2, \mu_0^2, Q_0^2) \longrightarrow \tilde{f}_s(N, k^2, Q_0^2) \quad (33)$$

$$\lim_{Q_0^2 \rightarrow 0} \tilde{f}_s(N, k^2, \mu_0^2, Q_0^2) \longrightarrow \tilde{f}_n(N, k^2, \mu_0^2). \quad (34)$$

The double cutoff case is slightly more work but one may also prove

$$\lim_{\substack{\mu_0^2 \rightarrow Q_0^2 \\ \mu_1^2 \rightarrow Q_1^2}} \tilde{f}_d(N, k^2, \mu_0^2, Q_0^2, \mu_1^2, Q_1^2) \longrightarrow \tilde{f}_d(N, k^2, Q_0^2, Q_1^2) \quad (35)$$

$$\lim_{\substack{\mu_1^2 \rightarrow \infty \\ Q_1^2 \rightarrow \infty}} \tilde{f}_d(N, k^2, \mu_0^2, Q_0^2, \mu_1^2, Q_1^2) \longrightarrow \tilde{f}_s(N, k^2, \mu_0^2, Q_0^2). \quad (36)$$

Having seen the above cross checks working analytically we now have confidence in our solutions and proceed to invert the remaining N -plane integral. To complete the inversion we need to perform the N -space integral :

$$f(x, k^2) = \int_{C_N} \frac{dN}{2\pi i} x^N \tilde{f}(N, k^2). \quad (37)$$

The contour, C_N , lies parallel to the imaginary axis and to the left of all singularities in the N -plane the nearest of which is the square root branch cut at $N = -K_0$. Writing $N = N_R + iN_I$, (with N_R fixed along the contour, C_N) the x^N factor may be written

$$x^N = x^{N_R} [\cos(N_I \ln(x)) + i \sin(N_I \ln(x))]$$

which tells us that the integrand is oscillating along the contour with period $2\pi/\ln x$.

Let us now consider the symmetry properties of the integrand under the transformation $N_I \rightarrow -N_I$. For any analytic function f which is real on some part of the real axis (which is true for the functions we will be considering) we have by the Schwartz reflection principle:

$$\begin{aligned} f(N_R + iN_I) &= \Re e(f(N_R + iN_I)) + i\Im m(f(N_R + iN_I)) \\ \Re e(f(N_R - iN_I)) &= \Re e(f(N_R + iN_I)) \\ \Im m(f(N_R - iN_I)) &= -\Im m(f(N_R + iN_I)). \end{aligned}$$

We see that the imaginary part of the integrand in eq.(37) is odd overall and the contributions from above and below the real axis cancel to produce a purely real function for the gluon density. So we have

$$f(x, k^2) = 2x^{N_R} \int_0^\infty \frac{dN_I}{2\pi} \left[\cos(N_I \ln x) \Re e(\tilde{f}) - \sin(N_I \ln x) \Im m(\tilde{f}) \right] \quad (38)$$

The non-trivial N -plane singularity structure associated with the square root branch points at $N = -K_0$ and $N = 0$ contained in the factor $1/2\omega_{N1}$ necessitates a numerical inversion of the remaining transform. We achieve this using a Fortran program which calls the NAG integration routine D01ASF which is specifically designed for integrals with oscillating integrands. Having performed the N -plane integral we have explicitly checked the smooth matching conditions for all ranges of k^2 and x .

The small- x behaviour, in the non-cutoff and infra-red cases, is dominated by the square root branch point at $N = -K_0$ (c.f. eq.(12)). In the double cutoff case the singularity structure in the N -plane is governed by $\Delta(\omega_{N1}) = 0$ defined in eq.(19), the zeros of this function occur at pure imaginary values of ω_{N1} and also at $\omega_{N1} = 0$ [4, 7]. In [4] it was shown that for the double-cutoff case this branch point singularity cancels between terms to leave a softer behaviour given by a sum of poles to the right of K_0 in the N -plane.

It appears from eq.(29) that we now have a singularity in $\tilde{f}_d(N, k^2)$ at $N = -K_0$ associated with the $1/2\omega_{N1}$ factor. A careful consideration of the terms in

square brackets, in the limit $\omega_{N1} \rightarrow 0$, however reveals that this singularity is cancelled and one is left with the sum of poles in the N -plane coming from the zeros of $\Delta(\omega_{N1})$ for which ω_{N1} are imaginary as before [4, 7].

3 Using the full BFKL kernel

In this section we explain how to implement a more realistic model which uses the analytic form for the full BFKL kernel given by eq.(8) ($K(\omega) = \bar{\alpha}_s \chi(\omega)$). Initially we include only the nearest poles at $\pm 1/2$ in the kernel. These are referred to as the leading twist poles since, as we will see, they lead to the largest power in Q^2 . The pole positions in the ω -plane, at $\pm \omega_{N1}$, are given by the solution to the following simultaneous equations

$$\begin{aligned} N_R + \Re(K(\omega_{N1})) &= 0 \\ N_I + \Im(K(\omega_{N1})) &= 0 \end{aligned} \tag{39}$$

such that

$$|\Re(\omega_{N1})| < \frac{1}{2} \tag{40}$$

The exact position of these poles depends on the choice of position of the contour in the N -plane, and on the position along this contour. Looking at the graph of $\Re(K(\omega))$ in fig.(1) we see that the solutions of the real part of the equation are given by a curves of constant height, $-N_R$, such that $-N_R > K_0$, where K_0 is the height of the saddle point at $\omega = (0, 0)$ (imagine taking a horizontal slice through the saddle). Provided this condition is satisfied, N_R lies to the left of all singularities in the N -plane. As N_I varies the solutions $\pm \omega_{N1}$ move along these curves. Having chosen the position of the N -plane contour we find ω_{N1} numerically, the complex solution then feeds into the residue of the poles calculated below.

We may now invert the solutions (7,15,17) to (N, k^2) -space, by closing the contour in the appropriate direction and summing over the residues of the enclosed poles as before. To do this we need to determine the contribution that the crucial

factor, $1 + N^{-1}K(\omega)$, makes to the residue. For example, if a particular term contains a closure factor forcing closure to the left we need to know the residue of the pole at $\omega = -\omega_{N1}$, so we expand the factor about this pole to arrive at

$$\begin{aligned}\frac{1}{1 + N^{-1}K(\omega)} &= \frac{\mathcal{R}(\omega)}{(\omega + \omega_{N1})} \\ \mathcal{R}^{-1} &= \left. \frac{\partial}{\partial \omega} \left(1 + \frac{\bar{\alpha}_s}{N} \chi(\omega) \right) \right|_{\omega = -\omega_{N1}} \\ \mathcal{R}(-\omega_{N1}) &= \frac{1}{(\bar{\alpha}_s/N) \chi'(-\omega_{N1})} \\ \chi'(\omega) &= \frac{\partial \chi(\omega)}{\partial \omega}\end{aligned}\tag{41}$$

with similar relations for the pole at $\omega = \omega_{N1}$. The function $\chi(\omega)$ which retains the full ω -dependence of the kernel is given by eq.(8)

For the non-cutoff case, closing to the left for $k^2 > \mu_0^2$, we have

$$\tilde{f}_n(N, k^2) = \frac{AN}{(N + \epsilon)} \left(-\frac{k^{2(1/2+\omega_0)}}{(N + K(\omega_0))} + \frac{k^{2(1/2-\omega_{N1})} \mu_0^{2(\omega_0+\omega_{N1})}}{(\omega_0 + \omega_{N1}) \bar{\alpha}_s \chi'(-\omega_{N1})} \right) \tag{42}$$

and to the right for $k^2 < \mu_0^2$,

$$\tilde{f}_n(N, k^2) = \frac{AN}{(N + \epsilon)} \left(\frac{k^{2(1/2+\omega_{N1})} \mu_0^{2(\omega_0-\omega_{N1})}}{(\omega_0 - \omega_{N1}) \bar{\alpha}_s \chi'(-\omega_{N1})} \right). \tag{43}$$

With an infra-red cutoff on the evolution, Q_0^2 , we get

$$\begin{aligned}\tilde{f}_s(N, k^2) &= \frac{AN}{(N + \epsilon)} \left(-\frac{k^{2(1/2+\omega_0)}}{(N + K(\omega_0))} + \frac{k^{2(1/2-\omega_{N1})}}{\bar{\alpha}_s \chi'(-\omega_{N1})} \times \right. \\ &\quad \left. \left[\frac{\mu_0^{2(\omega_0+\omega_{N1})}}{(\omega_0 + \omega_{N1})} - \frac{(\frac{1}{2} - \omega_{N1}) \mu_0^{2(\omega_0-\omega_{N1})} Q_0^{2(2\omega_{N1})}}{(\frac{1}{2} + \omega_{N1})(\omega_0 - \omega_{N1})} \right] \right) \end{aligned} \tag{44}$$

for $k^2 > \mu_0^2 > Q_0^2$. For $\mu_0^2 > k^2 > Q_0^2$ the input term is closed to the right to give

$$\begin{aligned}\tilde{f}_s(N, k^2) &= \frac{AN}{(N + \epsilon)} \frac{\mu_0^{2(\omega_0-\omega_{N1})}}{\bar{\alpha}_s \chi'(-\omega_{N1})} \times \\ &\quad \left(\frac{k^{2(1/2+\omega_{N1})}}{(\omega_0 - \omega_{N1})} - \frac{(\frac{1}{2} - \omega_{N1}) k^{2(1/2-\omega_{N1})} Q_0^{2(2\omega_{N1})}}{(\frac{1}{2} + \omega_{N1})(\omega_0 - \omega_{N1})} \right). \end{aligned} \tag{45}$$

Similarly the double cutoff case solution is given by

$$\tilde{f}_d(N, k^2) = \frac{AN}{(N + \epsilon)} \left(-\frac{k^{2(1/2+\omega_0)}}{(N + \epsilon)(N + K(\omega_0))} + \frac{1}{\bar{\alpha}_s \chi'(-\omega_{N1})} \right)$$

$$\begin{aligned}
& \times \left[\frac{\mu_0^{2(\omega_0+\omega_{N1})} k^{2(1/2-\omega_{N1})}}{(\omega_0+\omega_{N1})} - \frac{\mu_1^{2(\omega_0-\omega_{N1})} k^{2(1/2+\omega_{N1})}}{(\omega_0-\omega_{N1})} \right] \\
& + \frac{k^{2(1/2+\omega_{N1})} Q_1^{2(-\omega_{N1})} X_2(\omega_{N1}) - k^{2(1/2-\omega_{N1})} Q_0^{2(\omega_{N1})} X_1(\omega_{N1})}{\bar{\alpha}_s \chi'(-\omega_{N1}) \Delta(\omega_{N1}) (\frac{1}{2} + \omega_{N1})} \Big)
\end{aligned} \tag{46}$$

for $Q_1^2 > \mu_1^2 > k^2 > \mu_0^2 > Q_0^2$,

$$\begin{aligned}
\tilde{f}_d(N, k^2) &= \frac{AN}{(N+\epsilon) \bar{\alpha}_s \chi'(-\omega_{N1})} \left(\frac{k^{2(1/2+\omega_{N1})} (\mu_0^{2(\omega_0-\omega_{N1})} - \mu_1^{2(\omega_0-\omega_{N1})})}{(\omega_0-\omega_{N1})} \right. \\
&+ \left. \frac{k^{2(1/2+\omega_{N1})} Q_1^{2(-\omega_{N1})} X_2(\omega_{N1}) - (k^2)^{1/2-\omega_{N1}} Q_0^{2(\omega_{N1})} X_1(\omega_{N1})}{\Delta(\omega_{N1}) (\omega_{N1} + \frac{1}{2})} \right)
\end{aligned} \tag{47}$$

for $Q_1^2 > \mu_1^2 > \mu_0^2 > k^2 > Q_0^2$, and

$$\begin{aligned}
\tilde{f}_d(N, k^2) &= \frac{AN}{(N+\epsilon) \bar{\alpha}_s \chi'(-\omega_{N1})} \left(\frac{k^{2(1/2-\omega_{N1})} (\mu_0^{2(\omega_0+\omega_{N1})} - \mu_1^{2(\omega_0+\omega_{N1})})}{(\omega_0+\omega_{N1})} \right. \\
&+ \left. \frac{k^{2(1/2+\omega_{N1})} Q_1^{2(-\omega_{N1})} X_2(\omega_{N1}) - k^{2(1/2-\omega_{N1})} Q_0^{2(\omega_{N1})} X_1(\omega_{N1})}{\Delta(\omega_{N1}) (\omega_{N1} + \frac{1}{2})} \right)
\end{aligned} \tag{48}$$

for $Q_1^2 > k^2 > \mu_1^2 > \mu_0^2 > Q_0^2$.

Note that in these equations only terms corresponding to the input distribution change in the different k^2 -regimes. So the first and second terms in eqs.(44, 46) are the same as eq.(42); the first terms in eqs.(45, 47) are the same as eq.(43). The third term in eq.(46) and the second in eq.(47) (i.e. those involving μ_1^2) are present because a different input is used in the double cutoff case. The remaining terms in eqs.(44, 45, 46, 47) represent the effect of the cutoffs on the evolution.

The remaining N -plane integral is now performed numerically as described above employing extra subroutines in the Fortran programs to calculate $K(\omega_0)$ and $\chi'(\omega_{N1})$. Again we verify that the numerical solutions have the expected properties, i.e. that they satisfy the various limits detailed above. This has been done for $k^2 > \mu_0^2$ and $k^2 < \mu_0^2$ corresponding to the inversion of eqs.(42, 44, 46) and eqs.(43, 45, 47) respectively and we find that all the appropriate cross checks are observed.

Fig.(2) shows the effective small- x slope, λ_{eff} , defined by

$$\lambda_{\text{eff}} \equiv \frac{\partial \ln G(x, Q^2)}{\partial \ln 1/x}. \quad (49)$$

in each case, as a percentage of its asymptotic value of $\lambda_0 = 4 \ln 2 \bar{\alpha}_s$. Two curves are shown for the double cutoff case corresponding to the range of variables expected from HERA kinematics. The two values chosen for Q_1^2 , 10^3 and 10^5 GeV^2 , correspond (somewhat arbitrarily) to the maximum value of Q^2 at $x = 10^{-2}$ and the total centre-of-mass energy respectively.

3.1 Higher twist terms in the leading $\ln(1/x)$ approximation.

We now consider including further poles associated with the BFKL kernel. As explained above these poles are subleading in Q^2 and may be referred to as “higher twist” terms. Since the solutions get very complicated with more poles included, we restrict ourselves to the non-cutoff and infra-red cutoff cases as these contain the essential features.

Keeping the nearest and next-to-nearest poles in the kernel ($w = \pm 1/2, 3/2$) leads to four solutions of eq.(10) at $\omega = \pm\omega_{N1}, \pm\omega_{N2}$ where

$$1 < |\Re(\omega_{N2})| < \frac{3}{2}, \quad (50)$$

this can easily be seen from fig.(1) which shows the full kernel out to $\omega = \pm 3/2$. We note that $\Re(\omega_{N2}) \approx \Re(\omega_{N1}) + 1$.

The essential features can be illustrated using the following simple four pole kernel which has the same pole structure as the full kernel close to the contour:

$$K(\omega) = \frac{K_1}{(1 - 4\omega^2)} + \frac{K_2}{(9 - 4\omega^2)}. \quad (51)$$

where K_1, K_2 are determined, for example, by matching this kernel onto the full kernel (eq.(8)) at $\omega = 0, \pm 1$. Eq.(10) now has four solutions given by the solutions to a quartic equation in ω_N . The residue factor at these poles is given by (c.f. eq.(41))

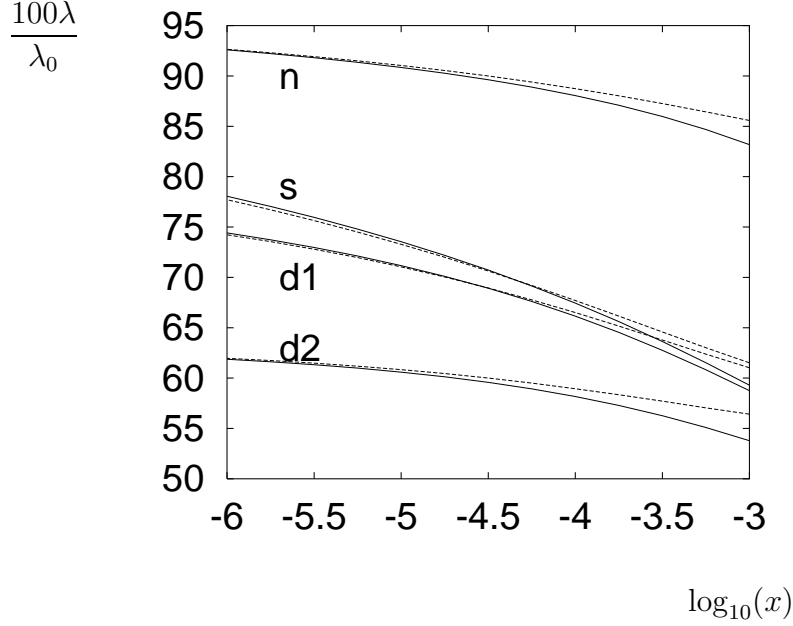


Figure 2: The effective slope of $G(x, Q^2)$ as a percentage of its asymptotic value $\lambda_0 = 4 \ln 2 \bar{\alpha}_s$, for $Q^2 = 10 \text{ GeV}^2$. The solid line in each pair of curves is for $\omega_0 = -1.0$ and the dashed line for $\omega_0 = -2.0$. At small enough x the slopes approach a value independent of the specific choice of ω_0 . For the curves shown in the single cutoff case (labelled 's'), $Q_0^2 = 0.5 \text{ GeV}^2$. In the double cutoff case we show two sets of curves; for $d1$, $Q_1^2 = 10^5 \text{ GeV}^2$ whereas for $d2$, $Q_1^2 = 10^3 \text{ GeV}^2$. μ_1^2 is set very high (10^9 GeV^2) so that the comparison can be made for the same input distribution (here $\mu_0^2 = 0.5 \text{ GeV}^2$).

$$\mathcal{R}(\omega_N) = \frac{(4\omega_N^2 - 1)(4\omega_N^2 - 9)}{8\omega_N [K_1(4\omega_N^2 - 9) + K_2(4\omega_N^2 - 1)]} \quad (52)$$

which becomes singular either when $\omega_N = 0$ or when the term in square brackets in the denominator becomes zero. For the leading poles at $\omega = \pm\omega_{N1}$ the former condition is satisfied when $N = -K_0 = -4 \ln 2\bar{\alpha}_s$ i.e at the original branch point. For the subleading poles in the ω -plane at $\omega_N = \pm\omega_{N2}$ the latter condition may be satisfied, this occurs for two complex conjugate values of $N \approx -K_0(0.1 \pm 0.25)$. Since these singularities lie far to the right of the branch point in the N -plane at $N = -K_0$ one expects them to be insignificant for small enough x .

This analysis may be extended trivially to include further poles in the kernel. The pole structure of the kernel determines that the solutions to $N + K(\omega_{N1}) = 0$ are spaced approximately one unit apart in terms of $\Re(\omega_{N1})$. This leads, on closing the ω plane contour, to a sum of k^2 terms with each subsequent term being approximately one power in k^2 down on the previous one (or equivalently in Q^2 once the k^2 integral has been performed). In this sense all the terms after the first one are higher twist in the language of the operator product expansion and may be neglected for large enough values of Q^2 . In what follows we investigate, and attempt to quantify, the magnitude of the contribution made by these additional poles at intermediate values of Q^2 and x , by explicitly including four poles in the BFKL kernel. This will be referred to as the next-to-leading pole calculation and denoted with a superscript “nl” (with a superscript “l” now for the leading pole solutions).

The non-cutoff case solution is straightforward. The effect of including this pole is to introduce terms in eqs.(42,43) in ω_{N2} identical in form to the existing terms in ω_{N1} , which are, approximately speaking, of order k^2/μ_0^2 relative to the leading, $k^{2(1/2-\omega_{N1})}$, terms.

Following the procedure outlined in [7], in the infra-red cutoff case the function $\mathcal{S}_s(N, \omega)$ is determined by the fact that it removes the right half plane poles (at $\omega = \omega_{N1}, \omega_{N2}$) from \mathcal{F}_s . Assuming a form which has the appropriate closure factor

$$\mathcal{S}(N, \omega) = Q_0^{-2\omega} \left(\frac{a_1}{\omega - \frac{1}{2}} + \frac{a_2}{\omega - \frac{3}{2}} \right),$$

one solves the following simultaneous equations:

$$\begin{aligned}\mathcal{F}^{(0)}(N, \omega_{N1}) + \mathcal{S}(N, \omega_{N1}) &= 0 \\ \mathcal{F}^{(0)}(N, \omega_{N2}) + \mathcal{S}(N, \omega_{N2}) &= 0\end{aligned}$$

to give

$$\begin{aligned}a_1 &= \frac{(1/2 - \omega_{N1})(1/2 - \omega_{N2})}{(\omega_{N1} - \omega_{N2})} \\ &\times \left[(3/2 - \omega_{N1})Q_0^{2\omega_{N1}}\mathcal{F}^{(0)}(N, \omega_{N1}) - (3/2 - \omega_{N2})Q_0^{2\omega_{N2}}\mathcal{F}^{(0)}(N, \omega_{N2}) \right] \\ a_2 &= \frac{(3/2 - \omega_{N1})(3/2 - \omega_{N2})}{(\omega_{N2} - \omega_{N1})} \\ &\times \left[(1/2 - \omega_{N1})Q_0^{2\omega_{N1}}\mathcal{F}^{(0)}(N, \omega_{N1}) - (1/2 - \omega_{N2})Q_0^{2\omega_{N2}}\mathcal{F}^{(0)}(N, \omega_{N2}) \right].\end{aligned}\tag{53}$$

We can now see that both a_1 and a_2 contain information about both the leading and next-to-leading poles. As we will see, this has a significant effect on the x dependence of the solution.

After inverting the ω -plane transform as appropriate for the values of k^2 (using the full kernel, $K(\omega) = \bar{\alpha}_s\chi(\omega)$, of eq.(8)) we arrive at the following solutions:

$$\begin{aligned}\tilde{f}_s(N, k^2) &= \frac{AN}{(N + \epsilon)} \left(-\frac{k^{2(1/2+\omega_0)}}{(N + K(\omega_0))} + \frac{k^{2(1/2-\omega_{N1})}}{\bar{\alpha}_s\chi'(-\omega_{N1})} \times \right. \\ &\quad \left. \left[\frac{\mu_0^{2(\omega_0+\omega_{N1})}}{(\omega_0 + \omega_{N1})} - Q_0^{2\omega_{N1}} \left(\frac{a_1}{(1/2 + \omega_{N1})} + \frac{a_2}{(3/2 + \omega_{N1})} \right) \right] \right) \\ &+ (\omega_{N1} \rightarrow \omega_{N2})\end{aligned}\tag{54}$$

for $k^2 > \mu_0^2 > Q_0^2$. For $\mu_0^2 > k^2 > Q_0^2$ we have

$$\begin{aligned}\tilde{f}_s(N, k^2) &= \frac{AN}{(N + \epsilon)} \times \left(\frac{k^{2(1/2+\omega_{N1})}}{\bar{\alpha}_s\chi'(-\omega_{N1})} \frac{\mu_0^{2(\omega_0-\omega_{N1})}}{(\omega_0 - \omega_{N1})} \right. \\ &\quad \left. - \frac{k^{2(1/2-\omega_{N1})}}{\bar{\alpha}_s\chi'(-\omega_{N1})} Q_0^{2\omega_{N1}} \left[\frac{a_1}{(1/2 + \omega_{N1})} + \frac{a_2}{(3/2 + \omega_{N1})} \right] \right) \\ &+ (\omega_{N1} \rightarrow \omega_{N2})\end{aligned}\tag{55}$$

Until now we have been working with the unintegrated gluon distribution function $f(x, k^2)$. This is not a physical observable. It must be convoluted with

an appropriate coefficient function to arrive at an observable for the particular process under consideration. For simplicity, we present our results in terms of the gluon structure function $G(x, Q^2)$ defined in eq.(1). Since we have analytic expressions for $\tilde{f}(N, k^2)$ in each case we may perform this k^2 integral prior to inverting the N -plane integral.

In the non-cutoff case we split the integral up into two regions and integrate eqs.(42,43),

$$\tilde{G}_n(N, Q^2) = \int_{\mu_0^2}^{Q^2} \frac{dk^2}{k^2} \tilde{f}_n(N, k^2) + \int_0^{\mu_0^2} \frac{dk^2}{k^2} \tilde{f}_n(N, k^2) \quad (56)$$

which gives for the leading pole solution

$$\begin{aligned} \tilde{G}_n^l(N, Q^2) &= \frac{AN}{(N + \epsilon)} \left(-\frac{(Q^{2(1/2+\omega_0)} - \mu_0^{2(1/2+\omega_0)})}{(\omega_0 + 1/2)(N + K(\omega_0))} \right. \\ &+ \frac{\mu_0^{2(1/2+\omega_0)}}{\bar{\alpha}_s \chi'(-\omega_{N1})} \left(\frac{1}{(1/2 + \omega_{N1})(\omega_0 - \omega_{N1})} - \frac{1}{(1/2 - \omega_{N1})(\omega_0 + \omega_{N1})} \right) \\ &+ \left. \frac{Q^{2(1/2-\omega_{N1})}}{\bar{\alpha}_s \chi'(-\omega_{N1})} \left(\frac{\mu_0^{2(\omega_0+\omega_{N1})}}{(1/2 - \omega_{N1})(\omega_0 + \omega_{N1})} \right) \right). \end{aligned} \quad (57)$$

The next-to-leading solution has an additional term relative to this

$$\begin{aligned} \tilde{G}_n^{nl}(N, Q^2) &= \tilde{G}_n^l(N, Q^2) + \frac{AN}{(N + \epsilon)} \times \\ &\left(\frac{\mu_0^{2(1/2+\omega_0)}}{\bar{\alpha}_s \chi'(-\omega_{N2})} \left(\frac{1}{(1/2 + \omega_{N2})(\omega_0 - \omega_{N2})} - \frac{1}{(1/2 - \omega_{N2})(\omega_0 + \omega_{N2})} \right) \right. \\ &+ \left. \frac{Q^{2(1/2-\omega_{N2})}}{\bar{\alpha}_s \chi'(-\omega_{N2})} \left(\frac{\mu_0^{2(\omega_0+\omega_{N2})}}{(1/2 - \omega_{N2})(\omega_0 + \omega_{N2})} \right) \right). \end{aligned} \quad (58)$$

In the single-cutoff case, which has the same input, the integral is non-zero in two regions:

$$\tilde{G}_s(N, Q^2) = \int_{\mu_0^2}^{Q^2} \frac{dk^2}{k^2} \tilde{f}_n(N, k^2) + \int_{Q_0^2}^{\mu_0^2} \frac{dk^2}{k^2} \tilde{f}_n(N, k^2) \quad (59)$$

the result differs from the non-cutoff solution only in the coefficient of $Q^{2(1/2-\omega_{N1})}$

$$\tilde{G}_s^l(N, Q^2) = \tilde{G}_n^l(N, Q^2) - \frac{AN}{(N + \epsilon)} \left(\frac{Q^{2(1/2-\omega_{N1})}}{\bar{\alpha}_s \chi'(-\omega_{N1})} \frac{\mu_0^{2(\omega_0-\omega_{N1})} (Q_0^2)^{2\omega_{N1}}}{(1/2 + \omega_{N1})(\omega_0 - \omega_{N1})} \right). \quad (60)$$

The next-to-leading solution can no longer be expressed in terms of the leading solution plus an extra piece from the new pole as in eq.(58) as a result of the information about the position of *both* poles tied up in the coefficients a_1, a_2 . The solution is given by

$$\begin{aligned}\tilde{G}_s^{nl}(N, Q^2) &= \tilde{G}_n^{nl}(N, Q^2) - \frac{(Q^{2(1/2-\omega_{N1})} - Q_0^{2(1/2-\omega_{N1})})}{(1/2 - \omega_{N1})\bar{\alpha}_s\chi'(-\omega_{N1})} \times \\ &\quad Q_0^{2\omega_{N1}} \left[\frac{a_1}{1/2 + \omega_{N1}} + \frac{a_2}{3/2 + \omega_{N1}} \right] \\ &\quad - (\omega_{N1} \rightarrow \omega_{N2}).\end{aligned}\tag{61}$$

For completeness we also give the double cutoff solution for the leading pole case for the same k^2 -regimes as in the single cutoff case:

$$\begin{aligned}\tilde{G}_d^l(N, Q^2) &= \tilde{G}_n^l(N, Q^2) + \frac{AN}{(N + \epsilon)} \times (\\ &\quad \frac{Q^{2(1/2+\omega_{N1})}}{\bar{\alpha}_s\chi'(-\omega_{N1})} \left(\frac{\mu_1^{2(\omega_0-\omega_{N1})}}{(1/2 + \omega_{N1})(\omega_0 - \omega_{N1})} \right) \\ &\quad - \frac{Q_0^{2(1/2+\omega_{N1})}(\mu_0^{2(\omega_0-\omega_{N1})} - \mu_1^{2(\omega_0-\omega_{N1})})}{\bar{\alpha}_s\chi'(-\omega_{N1})(1/2 + \omega_{N1})(\omega_0 - \omega_{N1})} \\ &\quad + \frac{1}{\bar{\alpha}_s\chi'(-\omega_{N1})(1/2 + \omega_{N1})\Delta(\omega_{N1})} \\ &\quad \times \left[- \frac{(Q^{2(1/2-\omega_{N1})} - Q_0^{2(1/2-\omega_{N1})})Q_0^{2\omega_{N1}}X_1(\omega_{N1})}{(1/2 - \omega_{N1})} \right. \\ &\quad \left. + \frac{(Q^{2(1/2+\omega_{N1})} - Q_0^{2(1/2+\omega_{N1})})Q_1^{-2\omega_{N1}}X_2(\omega_{N1})}{(1/2 + \omega_{N1})} \right] \Bigg). \end{aligned}\tag{62}$$

We now compare the model with two poles in the kernel to that with four in order to determine the significance of these next-to-leading poles as a function of Q^2 and x . To this end we work with the following quantity (which is the percentage difference between the two solutions)

$$R(x, Q^2) = 100 \times \frac{G^{(nl)}(x, Q^2) - G^{(l)}(x, Q^2)}{G^{(l)}(x, Q^2)}.\tag{63}$$

From the above analysis we expect R_n to go to zero as $Q^2 \rightarrow \infty$ since the coefficients of the leading Q^2 piece (the term in $Q^{2(1/2-\omega_{N1})}$) are the same in each

case (see eqs.(57,58)). In contrast, the coefficients of the “leading twist” pieces for the single cutoff case are different (see eqs.(60,61)) so we expect R_s to tend to a constant (which will be determined by the choice of input parameters ω_0, μ_0^2, Q_0^2 ; the overall normalization cancels in the ratio). Figs.(3,4) illustrate these features for a specific choice of input parameters.

Let us now consider the x dependence of these solutions. We have seen from the simple four pole model of the kernel that the singularities in the N -plane associated with ω_{N2} are subleading compared to the branch point at $N = -K_0$. The non-cutoff solution contains terms which involve either ω_{N1} or ω_{N2} but not both, hence one expects that the significance of the next-to-leading poles will decrease as $x \rightarrow 0$. One can see from fig.(5) that this is indeed the case. In the single cutoff case however the effects of the poles are coupled in the coefficients a_1, a_2 , this makes the x dependence of R_s considerably less trivial since the coefficient of the leading piece in x in $G_s^{(nl)}$ and $G_s^{(l)}$ are different.

Fig.(6) shows R_s as a function of x , for various Q^2 and two different values of the input parameter ω_0 . $\omega_0 = -1.0$ is special in that it lies in the same interval in ω as ω_{N2} . The curves shown for $\omega_0 = -2.0$ are typical of those for which ω_0 lies outside of this interval (< -1.5). For the latter, R_s is seen to increase as x decreases eventually tending to a constant percentage (of the order of 10 %) as $x \rightarrow 0$.

It seems that for intermediate values of x when an infra-red cutoff is present the next-to-leading poles in the BFKL equation are significant and including only one of the subleading poles leads to a behaviour in x similar to what one would expect for the sum of two powers.

This conclusion follows given the fact that we have chosen to regulate the infra-red physics using a theta function cutoff on the integral in eq.(2) and a specific form (20) for the input distribution. It would certainly be interesting to establish whether it is true in general.

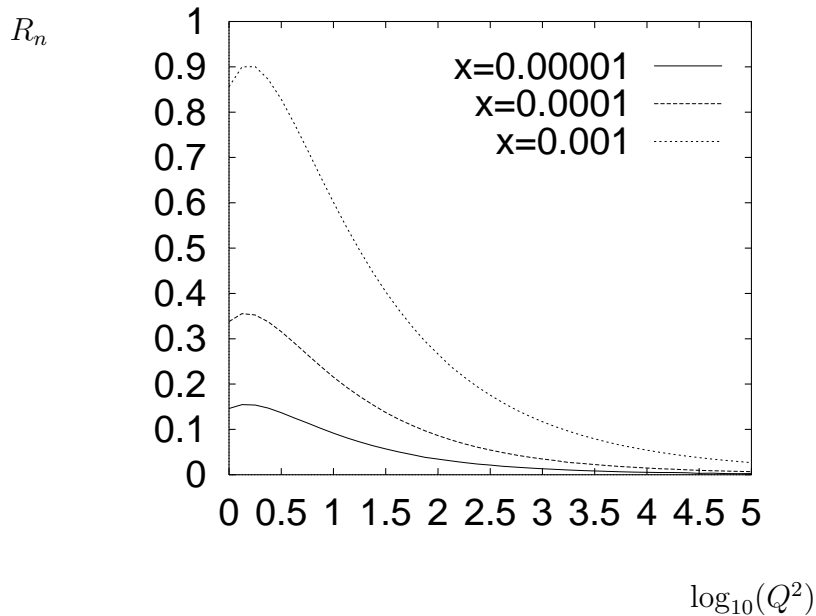


Figure 3: R_n as a function of Q^2 for various values of x showing that $R_n \rightarrow 0$ as $Q^2 \rightarrow \infty$. Here $\mu_0^2 = 0.5 \text{ GeV}^2$ and $\omega_0 = -2.0$.

Conclusions

We have presented analytic solutions to the BFKL equation with infra-red and ultra-violet cutoffs in moment space, including the leading pole of the full BFKL kernel. We have investigated the numerical significance of the subleading ('higher-twist') poles. We find that when one includes an infra-red cutoff the assumption that these poles are irrelevant is brought into question.

Acknowledgements

One of us (M.M.) would like to thank Graham Ross for supervision and discussions, Jochen Bartels for discussions and P.P.A.R.C. for financial assistance.

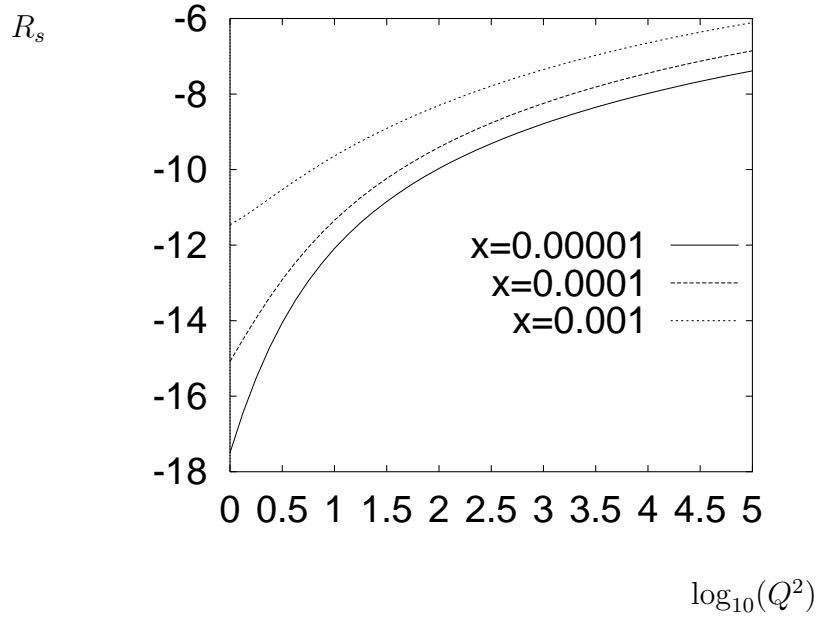


Figure 4: R_s as a function of Q^2 for various values of x . R_s tends to a constant as $Q^2 \rightarrow \infty$. Here $\mu_0^2 = 0.5 \text{ GeV}^2$, $Q_0^2 = 0.5 \text{ GeV}^2$ and $\omega_0 = -2.0$.

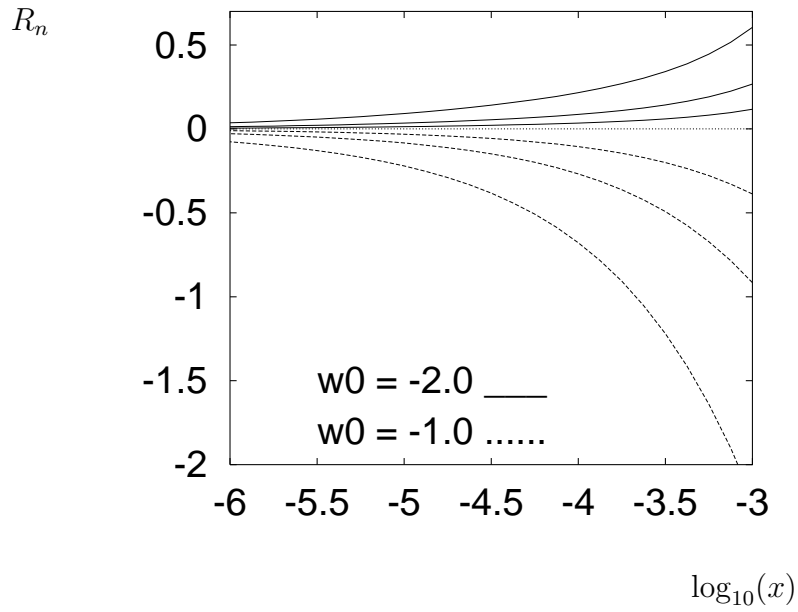


Figure 5: R_n as a function of x for various values of Q^2 . The percentage difference between the two solutions is less than 2% and tends to zero as $x \rightarrow 0$. The curves shown correspond to (largest first) $Q^2 = 10, 100, 1000$ GeV^2 . Here $\mu_0^2 = 0.5 \text{ GeV}^2$.

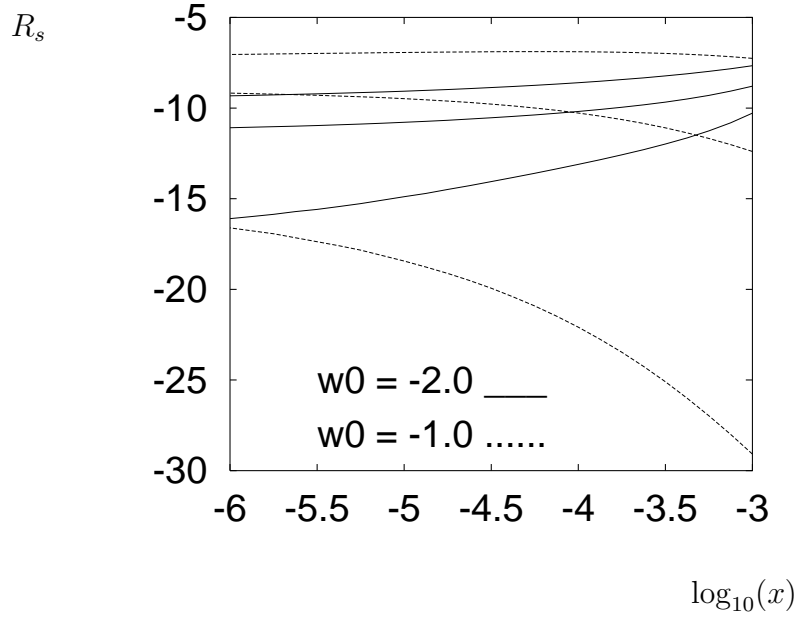


Figure 6: R_s as a function of x for various values of Q^2 . For the solid curves $\omega_0 = -2.0$, whereas for the dashed curves $\omega_0 = -1.0$. In each case the curves correspond to (largest first) $Q^2 = 1, 10, 100$ GeV². The input parameters are $\mu_0^2 = 0.5$ GeV², $Q_0^2 = 0.5$ GeV².

References

- [1] E.A. Kuraev, L.N. Lipatov and V.Fadin, Zh. Eksp. Teor. Fiz **72** (1977) 373; Sov. Phys. JETP **45** (1977) 199; Ya.Ya. Balitskij and L.N.Lipatov, Yad.Fiz. **28** (1978) 1597; Sov. J. Nucl. Phys. **28** (1979) 822; L.N.Lipatov, in “Perturbative QCD”, ed. A.H. Mueller (World Scientific, Singapore, 1989) 411.
- [2] V.N. Gribov and L.N. Lipatov, Sov. J. Nucl. Phys. **15**, 438,675 (1972); G. Altarelli and G.Parisi, Nucl. Phys. **B126**, 298 (1977); Y.L. Dokshitzer, Sov. Phys. JETP **46**, 641 (1977).
- [3] A.J. Askew, J. Kwiecinski, A.D. Martin and P.J. Sutton, Phys. Rev. **D47** (1993) 3775; Phys. Rev. **D49** (1994) 4402.
- [4] J.C. Collins and P.V.Landshoff, Phys. Lett. **B276** (1992) 196.
- [5] R.E. Hancock and D.A. Ross, Nucl. Phys. **B383** (1992) 575.
- [6] J.R. Forshaw, P.N. Harriman and P.J. Sutton, J.Phys G19 (1993) 1616; Nucl. Phys. **B416** (1994) 739.
- [7] M.F. McDermott, J.R. Forshaw and G.G. Ross, Phys. Lett. **B349** (1995) 189.
- [8] S. Catani and F. Hautmann, Nucl. Phys. **B427**, (1994), 475.
- [9] J.R. Forshaw, R.G. Roberts and R.S. Thorne, Phys. Lett. **B356** (1995) 79.
- [10] S. Catani, M. Ciafaloni, and F. Hautmann, Nucl. Phys. **B366**, 135 (1991); Phys. Lett. **B242**, 97 (1990).
- [11] R.D. Ball, S. Forte, Phys. Lett. **B335** (1994) 77; Phys. Lett. **B336** (1994) 77; Phys. Lett. **B351**, 313 (1995); M. Gluck, E.Reya and A.Vogt, Phys. Lett. **B306** (1993) 391; R.K.Ellis, Z.Kunszt and E.M.Levin, Nucl.Phys. **B420** (1994) 517.
- [12] J. Kwiecinski and A.D. Martin, Phys. Lett. **B353** (1995) 123.

[13] A. Donnachie and P.V. Landshoff, Phys. Lett. **B296**, 227 (1992).